Chemistry & Biology, Vol. 10, 139–147, February, 2003, ©2003 Elsevier Science Ltd. All rights reserved. DOI 10.1016/S1074-5521(03)00021-8

Crystal Structure of a Transition State Mimic for Tdp1 Assembled from Vanadate, DNA, and a Topoisomerase I-Derived Peptide

Douglas R. Davies,[1] Heidrun Interthal,[2] James J. Champoux,[2] and Wim G.J. Hol[1,3,*]
[1]Department of Biochemistry
[2]Department of Microbiology
School of Medicine
[3]Howard Hughes Medical Institute
University of Washington
Seattle, Washington 98195

Summary

Tyrosyl-DNA phosphodiesterase (Tdp1) is a member of the phospholipase D superfamily and acts as a DNA repair enzyme that removes stalled topoisomerase I-DNA complexes by hydrolyzing the bond between a tyrosine side chain and a DNA 3′ phosphate. Despite the complexity of the substrate of this phosphodiesterase, vanadate succeeded in linking human Tdp1, a tyrosine-containing peptide, and a single-stranded DNA oligonucleotide into a quaternary complex that mimics the transition state for the first step of the catalytic reaction. The conformation of the bound substrate mimic gives compelling evidence that the topoisomerase I-DNA complex must undergo extensive modification prior to cleavage by Tdp1. The structure also illustrates that the use of vanadate as the central moiety in high-order complexes has the potential to be a general method for capturing protein-substrate interactions for phosphoryl transfer enzymes, even when the substrates are large, complicated, and unusual.

Introduction

Tyrosyl-DNA phosphodiesterase (Tdp1) catalyzes the hydrolysis of a phosphodiester bond between a tyrosine side chain and a DNA 3′ phosphate [1]. Such a linkage is only known to occur in eukaryotic cells as part of the transient covalent enzyme-DNA intermediate formed when a type IB DNA topoisomerase nicks double-stranded DNA. Stalled topoisomerase I-DNA covalent complexes can be induced by various forms of DNA damage and by treatment with anticancer drugs such as camptothecin [2–4]. In the yeast *Saccharomyces cerevisiae*, Tdp1 has been shown to be involved in the repair of this type of DNA damage, since Tdp1 mutants become hypersensitive to camptothecin in situations where alternative pathways for DNA repair involving the checkpoint gene *RAD9* and the endonucleases *RAD1* and *MUS81* are blocked [5–8]. These findings suggest that inhibitors of Tdp1 may potentially be useful in combined drug therapy with camptothecin for treatment of cancers. The importance of human Tdp1 is also underlined by the recent discovery of a mutation in the enzyme that causes a hereditary neurological disorder called spinocerebellar ataxia with axonal neuropathy (SCAN1) [9].

Sequence comparisons and structural studies have shown that Tdp1 is a member of the phospholipase D (PLD) superfamily [10, 11]. Enzymes in this superfamily include PLDs, bacterial phosphatidyl serine and cardiolipin synthetases, a bacterial nuclease, a bacterial toxin, and a type II restriction endonuclease [12–15]. PLD superfamily enzymes catalyze phosphodiester bond cleavage through a phosphoryl transfer mechanism where the acceptor is either an alcohol or water. The similar chemistry for the members of the family appears to derive from a pair of motifs (referred to as "HKD motifs") where highly conserved histidine and lysine residues in the sequence HxK are necessary for catalytic activity [14, 16]. Structural studies have shown that pairs of HKD motifs come together to form a single active site [11, 16, 17]. Biochemical studies indicate that PLD superfamily enzymes catalyze reactions via two sequential S_N2 nucleophilic attacks, the first of which leads to formation of a covalent phosphohistidine intermediate, and the second of which cleaves the intermediate to yield the final products [10, 18–22].

Human Tdp1 is a monomeric protein that consists of two α-β-α domains that share similar topology, including a conserved seven-stranded mixed parallel-antiparallel β sheet [11] (Figure 1A). The active site containing the pairs of conserved histidine and lysine residues lies along a pseudo-2-fold axis of symmetry between the two domains. Structures of Tdp1 complexed with vanadate and tungstate showed these transition metal oxoanions to be covalently linked to His263, confirming this residue as the nucleophile in the first step of the catalytic reaction [23]. The active site is centrally located in an asymmetrical cleft that extends approximately 40 Å across the surface of the enzyme. On one side of the active site, this narrow 8 Å wide cleft has a predominantly positively charged electrostatic surface potential. On the other side of the active site, the cleft widens into a semiconically shaped depression that is approximately 20 Å wide at the end distal to the active site and is lined with a mixture of both basic and acidic amino acid residues. The shape and charge distribution of these substrate binding clefts, together with clues provided by the Tdp1-vanadate structure, led to the hypothesis that the narrow positively charged cleft binds the DNA moiety of the substrate and that the wider cleft binds the peptide moiety [11, 23].

The nucleic acid-protein substrate of Tdp1 is complex. The native human topoisomerase I-DNA complex consists of a 91 kDa protein covalently bound to a nicked, double-stranded DNA molecule. A crystal structure of a reconstituted human topoisomerase I covalently bound to double-stranded DNA shows that the scissile phosphotyrosine bond is buried deep within this complex and would be inaccessible to Tdp1 (see Figure 2A) [24]. Indeed, a complex containing a native form of topoisomerase I is cleaved poorly if at all by human Tdp1 (H.I. and J.J.C., unpublished results). It has been

*Correspondence: hol@gouda.bmsc.washington.edu

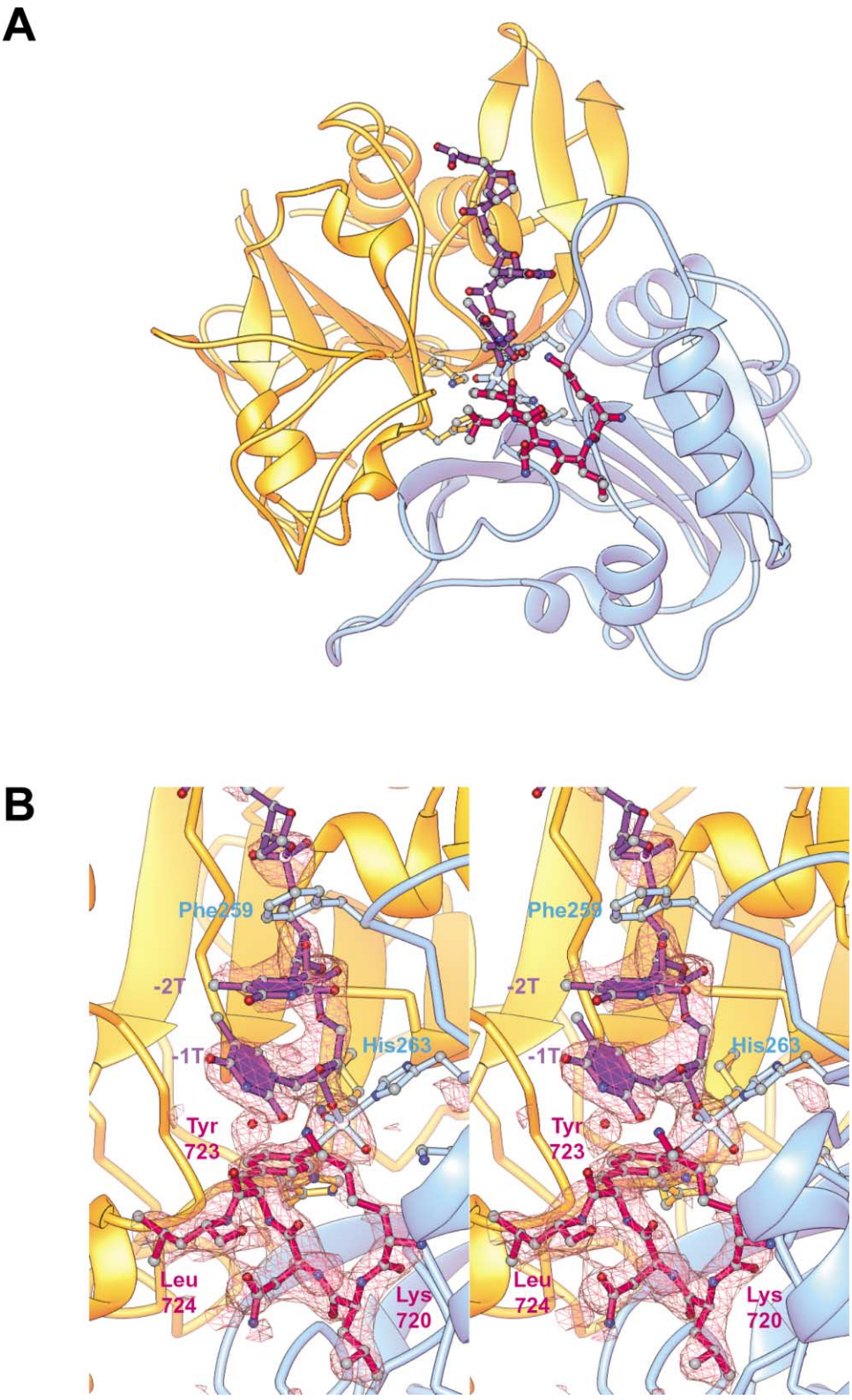

Figure 1. The Structure of the Tdp1-Vanadate-Peptide-DNA Complex

(A) Ribbon diagram for the overall structure. Tdp1 is displayed as a ribbon structure with the N-terminal domain (residues 162–350) colored blue and the C-terminal domain (residues 351–608) colored yellow, viewed down the pseudo-2-fold axis of symmetry between the domains. His263, Lys265, His493, and Lys495 are displayed as ball-and-stick structures. The substrate analog is also displayed in ball-and-stick form with the bonds of the peptide moiety in magenta, the vanadate in blue, and the DNA in purple.

(B) Difference electron density for the Tdp1-vanadate-peptide-DNA complex. Coloration is the same as in (A). The topoisomerase I-derived peptide follows the numbering system of the full-length topoisomerase I enzyme. Contours represent the 2.5-sigma level in the initial F_o-F_c electron density map calculated for the molecular replacement solution with apo-Tdp1 used as the search model. Figures 1, 2, and 3 were created using RIBBONS [34].

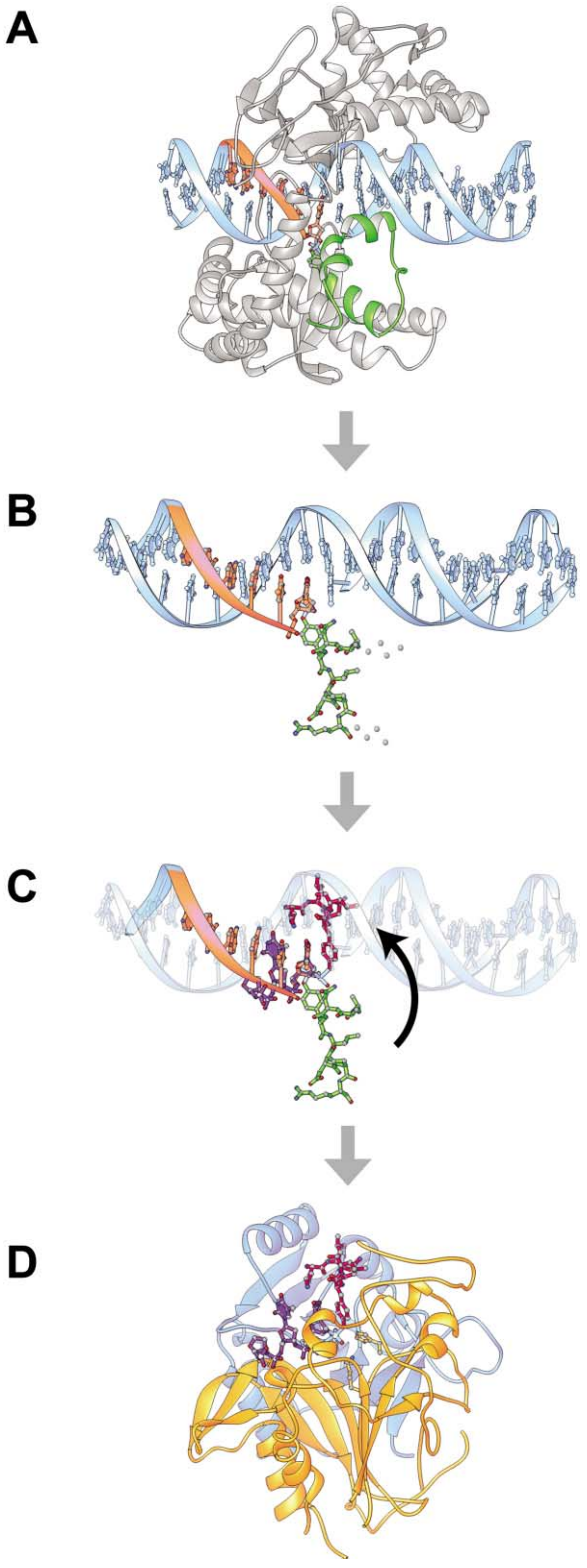

Figure 2. Comparison of the Topoisomerase I-DNA Covalent Complex with the Peptide-Vanadate-DNA Substrate Mimic Bound to Tdp1

(A) The crystal structure of a human topoisomerase I-DNA covalent complex [24]. This model represents catalytically active "reconstituted topoisomerase I" that consists of core subdomains I–III (residues 215–634, colored gray) and the C-terminal domain (residues 713–765, colored green) covalently bound to a cleaved 22-base pair DNA duplex (colored blue) via Tyr723. Not shown is a 69-residue coiled-coil domain present in the native enzyme that acts as a linker between the core subdomains and the C-terminal domain. Tyr723, the catalytic residue that forms the phosphotyrosine intermediate, is located in the C-terminal domain and is displayed as a green ball-and-stick structure. The −1 to −6 residues of DNA on the 5′ side of the phosphotyrosine linkage (corresponding to the length of the oligonucleotide used for crystallization with Tdp1) are colored orange.

(B) Model of the "native" conformation of the Tdp1 substrate, as observed in the crystal structure of a topoisomerase I-DNA covalent complex. For clarity, all protein except for the eight residues corresponding to the peptide moiety in the Tdp1-vandadate-peptide-DNA cocrystal complex (green ball-and-stick structure) has been removed, and the structure has been rotated slightly around the DNA axis from the view in (A). Dotted lines extending form the N and C termini of the peptide indicate that the actual size of the peptide that eventually binds to Tdp1 in vivo is not known.

(C) Comparison of the observed structures of DNA and topoisomerase I peptide from the native structure of the topoisomerase I-DNA covalent complex [24] (orange and green) and the Tdp1-vanadate-peptide-DNA complex (purple and magenta). The two structures are superimposed at the −1 nucleotide. The curved arrow shows the relative rotation of the peptide moiety from the conformation in the native topoisomerase I-DNA complex to the conformation observed bound to Tdp1. The conformation observed in the Tdp1 structure could not be achieved without removal or significant structural rearrangement of the intact strand and the 3′ end of the nicked strand of DNA in the topoisomerase I-DNA complex.

(D) The crystal structure of the Tdp1-vanadate-peptide-DNA complex. This view preserves the orientation of the substrate mimic that is displayed in (C). Tdp1 is depicted as a ribbon diagram with the same color scheme as in Figure 1 and is viewed nearly perpendicular to the pseudo-2-fold axis of symmetry.

suggested that the topoisomerase I-DNA complex must undergo modification or partial degradation prior to cleavage of the phosphotyrosine bond by Tdp1 [1].

Several clues about the nature of the Tdp1 substrate in vivo have recently emerged. Genetic studies in yeast have indicated that Tdp1 may function subsequent to the formation of the double-strand break that results from collision of a replication fork with a stalled topoisomerase I [6]. Consistent with this hypothesis, yeast Tdp1 has been shown to prefer substrates with a tyrosine residue at the 3′ end of either single-stranded DNA or blunt-ended duplexes over substrates with tyrosine on the 3′ end at a nick in the middle of a duplex [6]. Although a native topoisomerase I-DNA complex is not a substrate for Tdp1, a complex of DNA and the isolated 6.3 kDa C-terminal domain of topoisomerase I that contains the active tyrosine is cleaved (H.I. and J.J.C., unpublished results). Additional information about substrates that can be accepted by Tdp1 comes from the fact that in vitro experiments with human Tdp1 are routinely performed using a substrate called "12-pep," a fragment of the human topoisomerase I-DNA complex consisting of a single-stranded 12-mer oligonucleotide with a small trypsin-resistant peptide linked to the 3′ end of the DNA via the active site tyrosine [10].

The ability of human Tdp1 to cleave the 12-pep substrate, the shape of the putative DNA binding cleft, and lessons learned from the study of Tdp1-vanadate crystals suggested experiments to explore the feasibility of

inducing binding of a short peptide, a single strand of DNA, and vanadate simultaneously in the active site of Tdp1. By exploiting the versatile ligand binding properties of vanadate, a quaternary complex that mimics the transition state of the Tdp1-catalyzed reaction could be obtained. The crystal structure of this quaternary complex provides further insights into the catalytic mechanism and substrate binding properties of Tdp1.

Results and Discussion

The Quaternary Complex with Vanadate

In the previously determined crystal structure of Tdp1-vanadate, a glycerol molecule from the cryoprotectant solution formed a cyclic diester complex with the vanadate moiety [23]. Attempts to cocrystallize Tdp1 with vanadate and single-stranded oligonucleotides yielded similar structures of vanadate-glycerol complexes when glycerol was used as a cryoprotectant, but no DNA could be seen in the electron density maps (D.R.D., unpublished results). Most likely, the formation of complexes of Tdp1, vanadate, and substrates was hampered by interference from glycerol. Since the hydroxyl groups of glycerol might have been competing with the 3′OH of the DNA oligonucleotides as ligands for vanadate, subsequent cocrystallization experiments employed a cryoprotectant lacking free hydroxyl groups, PEG 250 dimethyl ether.

By using precise cocrystallization and cryoprotection protocols, enzyme, vanadate, peptide, and DNA were induced to self-assemble around a central vanadate moiety in the active site of Tdp1. The peptide (NH_2-Lys-Leu-Asn-Tyr-Leu-Asp-Pro-Arg-COOH) corresponds to residues 720–727 of human topoisomerase I, a segment of the C-terminal domain containing the active site tyrosine residue, Tyr723. The DNA oligonucleotide used was a 6-mer (5′-AGAGTT-3′) derived from the DNA sequence in the Tdp1 substrate 12-pep. Along with vanadate, the peptide and DNA cocrystallize with Tdp1 in the same space group with similar unit cell dimensions as Tdp1-vanadate and Tdp1-tungstate crystals [23]. The structure of the quaternary complex was solved by molecular replacement at a resolution of 2.3 Å (Figure 1). The ensuing difference electron density map clearly indicated that a covalent complex of Tdp1, vanadate, peptide, and ssDNA had been obtained (Figure 1B).

The vanadate at the center of the quaternary complex adopts a trigonal bipyramidal configuration that mimics the transition state of an S_N2 nucleophilic attack on phosphate (Figures 1B and 3A). One apical ligand is contributed by the Nε2 atom of His263 of Tdp1, and the other apical ligand is the oxygen atom of the tyrosine side chain of the topoisomerase I-derived peptide. One of the three equatorial oxygen ligands to vanadate is contributed by the 3′ hydroxyl of the DNA oligonucleotide. The remaining two equatorial oxygen ligands represent the nonbridging oxygens of the phosphodiester substrate, and each one is within hydrogen-bonding distance of the Nζ atom of a lysine and the Nδ2 atom of an asparagine (Figure 3A). These residues, Lys265, Asn283, Lys495, and Asn516, are conserved among Tdp1 orthologs and are likely important for substrate binding and transition state stabilization [10]. Linkage to vanadate indicates that His263 is the attacking nucleophile for the first step of the Tdp1 catalytic reaction. Therefore, the peptide moiety occupying the apical position opposite His263 represents the leaving group for this step. In its equatorial location, the DNA strand represents the portion of the phosphodiester substrate that would remain bound to Tdp1 via a covalent phosphohistidine linkage until hydrolysis of the phosphohistidine intermediate occurs in the second step of the catalytic reaction. The DNA is bound in the narrow, positively charged substrate binding groove, and the peptide is located in the wider substrate binding cleft (Figure 4), confirming our earlier prediction concerning the orientation of the bound peptide and DNA moieties of the substrate [23].

Substrate Binding Characteristics

The N-terminal five residues of the 8-mer peptide are visible in the electron density map (Figure 3B). The peptide moiety of the quaternary complex occupies a small portion of the wide substrate binding cleft, burying approximately 575 $Å^2$ of solvent-accessible surface area but makes only three direct hydrogen bonding contacts with Tdp1. Lys720 of the topoisomerase I-derived peptide contacts the carboxylate side chain of Asp230, the backbone nitrogen of Phe206, and the phenolic oxygen of Tyr204 (Figure 3B). However, Tyr204 and Asp230 are not conserved among Tdp1 orthologs. The conformation of the peptide, as seen in our quaternary complex, is significantly different from the conformation of the corresponding region found in the crystal structures of human topoisomerase I. Both the N and C termini of the topoisomerase I-derived peptide are oriented in such a way that additional stretches of polypeptide could be accommodated with little or no conformational change by either the peptide or Tdp1. Nevertheless, the structure of the topoisomerase I-derived peptide observed here may not reflect the conformation present in the natural Tdp1 substrate, where the peptide moiety may be substantially larger. Surprisingly, Tyr723 makes no contacts with Tdp1 whatsoever, aside from the covalent linkage to the enzyme via vanadate. This observed lack of specificity for tyrosine is consistent with a recent report that Tdp1 is also capable of removing glycolate from 3′-phosphoglycolate on DNA [25] and suggests that Tdp1 may have a broad specificity for a variety of blocked 3′ DNA termini.

In the structure, three nucleotides of the 6-mer DNA at the 3′ end of the oligonucleotide are visible in the electron density map, representing the −1 to −3 positions according to the topoisomerase I nomenclature, although the purine base moiety of −3G is disordered. These three nucleotides extend nearly to the end of the narrow, positively charged substrate binding cleft and bury approximately 400 $Å^2$ of solvent-accessible surface area (Figure 4). Out of ten direct and water-mediated hydrogen bonds between Tdp1 and DNA, all but one contact phosphate groups (Figure 3C). The remaining hydrogen bond is between the phenolic oxygen of Tyr204 of Tdp1 and the O2 atom of the thymine base at the −1 position. Interestingly, the same nucleotide

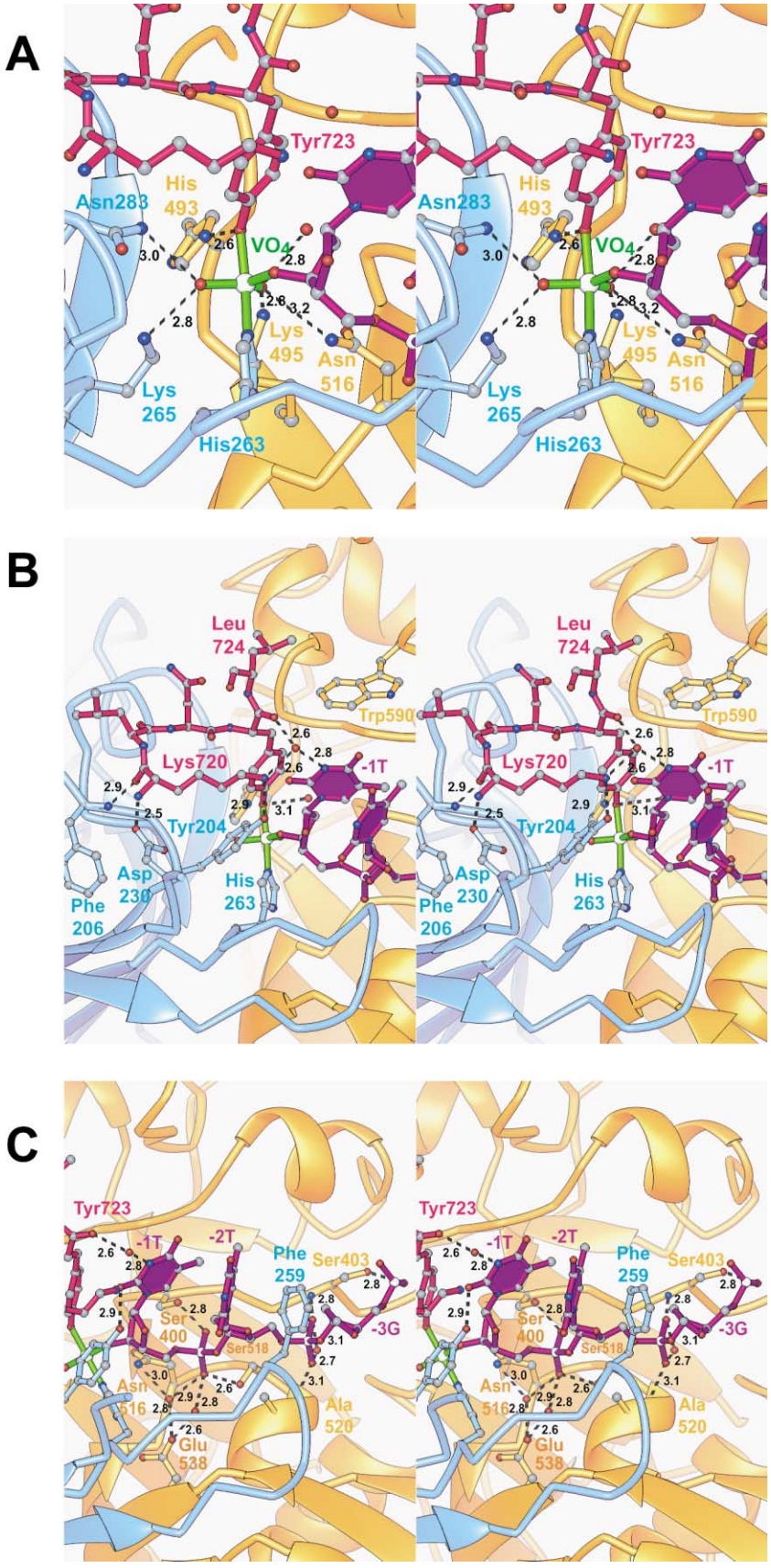

Figure 3. Hydrogen Bonding Contacts between Tdp1 and the Vanadate-Peptide-DNA Substrate Transition State Analog

Tdp1, peptide, and DNA are colored as in Figure 1A, with the vanadate moiety in green and hydrogen bonds indicated by dashed lines. Residues 232–242 of Tdp1 have been omitted for clarity. Hydrogen bonds to the vanadate moiety are displayed in (A), hydrogen bonds to the peptide moiety are displayed in (B), and hydrogen bonds to the DNA moiety in (C).

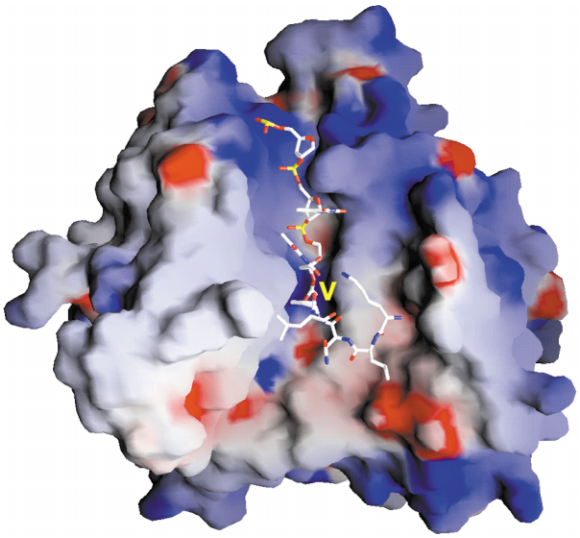

Figure 4. Electrostatic Potential Surface of Tdp1

The molecular surface is colored between −10kT (red) and +10kT (blue) and was generated with the program GRASP [35]. The orientation of the Tdp1 structure is the same as in Figure 1A. The peptide-vanadate-DNA substrate mimic is displayed as a stick structure. The yellow V indicates the position of the vanadate residue in the active site. The DNA moiety extends above the active site, bound in the narrow, positively charged half of the substrate binding groove. The peptide moiety is located below the active site in a relatively neutral portion of the wider substrate binding cleft.

oxygen atom is involved in the sole base-specific contact observed in the structures of human topoisomerase I bound to DNA and possibly reflects the sequence preference of the topoisomerase for a thymine base at the −1 position [26]. Otherwise, the relative lack of sequence specificity in DNA binding by Tdp1 is to be expected, since topoisomerase I has only weak sequence specificity [27, 28]. Thus, stalled complexes between DNA and topoisomerase I could occur with a variety of different DNA sequences.

Surprisingly, most of the Tdp1-DNA contacts are with polar but not basic residues despite the fact that the DNA binding cleft is positively charged. Phosphate binding sites containing serine appear to be a common motif among Tdp1 orthologs, as Ser400, Ser403, and Ser518 are conserved [10]. Notably, Ser400 and Ser518 are also conserved in the only two other PLD superfamily members besides Tdp1 known to have a DNA substrate: a nuclease from *Salmonella* and the BfiI restriction endonuclease [11, 15]. Interestingly, the 5′ phosphate of −2T occupies the same position that was identified as a low-occupancy tungstate binding site in the structure of Tdp1-tungstate [23]. Another conserved residue is Phe259 (conserved in all known species except *Schizosaccharomyces pombe*, where it is tryptophan), which is in position to intercalate between the bases at the −2 and −3 positions. Thus, Phe259, along with the conserved phosphate binding serine residues, expand the Tdp1 signature sequence that includes the pairs of HxK sequences (His263, Lys265, His493, and Lys495) and other conserved residues in the active site, Thr281, Asn283, Asp288, Gln294, Asn516, and Glu538 in the human enzyme [10, 23]. The identities and functions of the key residues in this expanded Tdp1 signature sequence are presented in Table 1.

The overall conformation of the DNA bound to Tdp1 is irregular and extended and is elongated compared to B-form DNA. Modeling studies indicate that canonical duplex DNA is unlikely to bind to Tdp1 in the absence of a conformational change in the nucleotides at the 3′ end, since the backbone of a strand of DNA forming Watson-Crick base pairs with nucleotides −1 to −3 would likely clash with loop 229–232 of Tdp1 (data not shown). However, since phosphotyrosine at the 3′ end of a blunt-ended DNA duplex has been shown to be a substrate for *S. cerevisiae* Tdp1 [6], the question remains if and how human Tdp1 can accommodate double-stranded DNA in its substrate binding groove. Given the narrow DNA binding cleft observed in the native enzyme [11] and the current quaternary complex, it would appear that in order for human Tdp1 to remove a topoisomerase I peptide from the end of duplex DNA, a conformational change in either Tdp1 or the DNA must occur. Unpairing of the terminal few base pairs of the duplex may be sufficient to allow binding by Tdp1.

Processing of the Topoisomerase I-DNA Complex Is Required Prior to Tdp1 Cleavage

The conformation of the analog of the topoisomerase I-DNA fragment bound to Tdp1 provides compelling evidence that the topoisomerase I-DNA complex must undergo extensive structural changes such as proteolysis and/or unfolding prior to cleavage by Tdp1 as suggested earlier by Yang et al. [1]. The relative conformations of the peptide and DNA moieties in the crystal structure of a topoisomerase I-DNA covalent complex and in the Tdp1 substrate binding clefts are remarkably different (Figure 2C). In the Tdp1 structure, the aromatic rings of the tyrosine of the peptide and the base at the −1 position of the DNA are in proximity to one another, although too widely spaced to exhibit stacking interactions. This arrangement is in contrast to the conformation observed in the covalent topoisomerase I-DNA structure, where the tyrosine ring and the base of nucleotide −1 adopt a "trans" conformation about the central phosphate moiety (Figure 2C). Remarkably, the conformation observed for the peptide-vanadate-DNA substrate analog bound to Tdp1 could not be achieved in an intact topoisomerase I-DNA complex involving duplex DNA, because the tyrosine would clash with the 5′ end of the nicked strand of DNA as seen in the topoisomerase I-DNA complex (Figures 2B and 2C). This finding is in agreement with the observation that the native 91 kDa topoisomerase I-DNA complex is refractory to cleavage by Tdp1 (H.I. and J.J.C., unpublished results). Some significant rearrangement of the topoisomerase I-DNA complex is therefore required in order for the substrate to adopt the conformation observed in the Tdp1 quaternary complex. Removal or unpairing of the intact strand of DNA coupled with proteolytic degradation or unfolding of the core subdomains of topoisomerase I are possible mechanisms that would allow the phosphodiester moiety enough conformational flexibility to bind to Tdp1 in the manner displayed in the crystal structure of the quaternary complex.

Table 1. Conserved Residues in Tdp1 Orthologs and Their Function

Residue in Human Sequence	Function
Phe259 (Trp in *S. pombe*)	DNA binding
His263	Nucleophile in first step of catalytic reaction
Lys265	Substrate binding and transition state stabilization
Thr281 (Ser in *S. cerevisiae*)	Orientation of Gln294
Asn283	Substrate binding and transition state stabilization
Asp288 (Glu in *S. cerevisiae*)	Orientation of Gln294
Gln294	Orientation of His493
Ser400	DNA binding
Ser403 (Thr in *T. brucei*)	DNA binding
His493	General acid-base catalyst
Lys495	Substrate binding and transition state stabilization
Asn516	Substrate binding and transition state stabilization
Ser518	DNA binding
Glu538	Activation of His263

Residues are defined as "conserved" based on a multiple sequence alignment of Tdp1 orthologs from human, *S. cerevisiae, S. pombe, D. melanogaster, C. elegans*, and *A. thaliana* [10] and from BLAST alignments of human Tdp1 with the Tdp1 orthologs from *T. brucei* (TIGR locus no. 1F7.245), *M. musculus* (accession no. XP_127061), and *A. gambiae* str. PEST (accession no. EAA09907).

The use of vanadate as a versatile phosphate mimic has revealed the structures of transition states in mechanisms such as ATP hydrolysis by myosin [29] and RNA hydrolysis by the hairpin ribozyme [30]. The complex of vanadate with Tdp1, peptide, and DNA is an even more comprehensive example of the utility of vanadate as a tool for structural investigations. To our knowledge, the Tdp1 structure presented here is the first time that vanadate has been used for the generation of a quaternary complex composed of vanadate and three additional distinct components. The quaternary complex of Tdp1 with vanadate is also significant in that it provides clues to the overall pathway of degradation of topoisomerase I-DNA complexes in addition to representing the transition state for a step in the catalytic reaction.

Significance

Tyrosyl-DNA phosphodiesterase (Tdp1) is a DNA repair enzyme involved in the repair of stalled topoisomerase I-DNA complexes. Tdp1, vanadate, single-stranded DNA, and a topoisomerase I-derived peptide self-assemble into a quaternary complex that reveals, in a single glance, the substrate binding mode and the mechanism of the first catalytic step for the enzyme. Single-stranded DNA is bound in the narrow, positively charged groove of the substrate binding cleft, although uncharged polar side chains are largely responsible for specific interactions with the DNA. The peptide moiety is bound in the larger, more open half of the substrate binding cleft but is held in place with very few specific hydrogen bonds. The trigonal bipyramidal geometry of the vanadate moiety is consistent with the transition state of an S_N2 nucleophilic attack on phosphate, where the tyrosine-containing peptide is the leaving group. Remarkably, the conformation of the substrate analog observed in the Tdp1 complex cannot be achieved without significant rearrangement or degradation of the native topoisomerase I-DNA complex, consistent with the previous proposal that additional factor(s) must participate in the Tdp1-mediated repair pathway.

This quaternary complex demonstrates the full potential of vanadate as a powerful aid in structure determination. To our knowledge, the transition state mimic for the Tdp1 reaction presented here is the first time that vanadate has been used for the generation of a quaternary complex composed of vanadate plus three distinct components in the context of a biological molecule. This use of vanadate is potentially a general method for obtaining structural information about interactions of phosphoryl transfer enzymes with substrates that would otherwise be difficult or expensive to synthesize or purify. Vanadate may also be useful as a tool for finding leads in structure-based inhibitor design for Tdp1 and other enzymes that carry out phosphoryl transferring reactions, as it can act as a covalent anchor capable of accepting a variety of test ligands.

Experimental Procedures

Crystallization

Human Tdp1 (Δ1-148) was purified as described [10]. An 8-amino-acid peptide of sequence NH_2-Lys-Leu-Asn-Tyr-Leu-Asp-Pro-Arg-COOH was synthesized by United Biochemical Research (Seattle, WA). This peptide corresponds to residues 720–727 of human topoisomerase I and contains the catalytic tyrosine residue, Tyr723. This peptide corresponds to the predicted sequence for the trypsin-resistant peptide moiety of the "12-pep" substrate [10] with the addition of an N-terminal lysine. The DNA employed was a 6-mer oligonucleotide of sequence 5′-AGAGTT-3′ synthesized by Macromolecular Resources (Fort Collins, CO). The sequence was derived from the 3′ end of the nucleic acid portion of the "12-pep" substrate used for Tdp1 activity assays [10]. Crystallization was carried out by mixing a solution of Tdp1 (5.5 mg/ml), 3 mM sodium orthovanadate, 5 nmol/μl DNA, and 20 nmol/μl peptide in 1 × 1 microliter sitting drops with a crystallant containing 22% PEG 3350, 100 mM HEPES (pH 7.8), 200 mM NaCl, and 10 mM spermine. Crystals belonged to space group $P2_12_12_1$, had a plate-like habit, and grew to approximately 0.2 × 0.1 × 0.02 mm in 2–4 days. Cell dimensions were a = 49.80 Å, b = 104.72 Å, c = 193.92 Å. Crystals were stabilized for flash cooling by direct transfer to a cryoprotectant containing 14% PEG 3000, 375 mM NaCl, 100 mM HEPES (pH 7.8), 28% PEG 250 dimethyl ether, 5 mM sodium orthovanadate, 5 nmol/μl DNA, and 20 nmol/μl peptide. After 30–60 s in cryoprotectant, crystals were flash cooled by direct plunging into liquid nitrogen.

Table 2. Data Collection and Refinement Statistics for Tdp1-Vanadate-DNA-Peptide

Data Collection	
λ (Å)	1.0332
Space group	$P2_12_12_1$
Unit cell dimensions a,b,c (Å)	49.80, 104.72, 193.92
Resolution (Å)	2.30
Mosaicity (°)	0.474
Unique reflections	41018
Completeness (highest shell) (%)	92.6 (61.9)
Average I/σ[a] (highest shell)	18.88 (2.08)
Redundancy	4.7
R_{sym} (%)[b]	8.5 (33.9)
Refinement	
Resolution range (Å)	100–2.3
Reflections (free)	38958 (2060)
$R_{crystal}$ (R_{free}) (%)[c]	20.6 (25.2)
Rms deviations from ideality	
Bond lengths (Å)	0.014
Bond angles (degrees)	1.387
Chirality	0.096

[a] I/σ is the mean reflection intensity divided by the estimated error.
[b] $R_{sym} = (\Sigma|I_{hkl} - <I>|)/(\Sigma I_{hkl})$, where the average intensity $<I>$ is taken over all symmetry equivalent measurements, and I_{hkl} is the measured intensity for any given reflection.
[c] $R_{crystal} = ||F_o| - |F_c||/|F_o|$, where F_o and F_c are the observed and calculated structure factor amplitudes, respectively. R_{free} is equivalent to $R_{crystal}$, but calculated for 5% of the reflections chosen at random and omitted from the refinement process.

Data Collection, Structure Solution, and Refinement

Data were collected at beamline 19-BM of the Advanced Photon Source on a 3 × 3 tiled CCD detector. Data were reduced with Denzo and scaled with Scalepack [31]. Phases were determined by molecular replacement with AMORE [32] using the crystal structure of Tdp1-vanadate as a search model. Crystals contained two monomers of Tdp1 per asymmetric unit, but only the A subunit included peptide and DNA bound at high occupancy, possibly due to crystal packing interactions. A view of the difference electron density map for the initial molecular replacement solution is shown in Figure 1B. For clarity, all descriptions and figures in this paper are based on the model of the A subunit in the crystal structure. Model building was performed using Xtalview [33], and the structure was refined using Refmac5 [32]. Data collection and refinement statistics are summarized in Table 2.

Acknowledgments

We gratefully acknowledge the staff of beamline 8.2.1 of the Advanced Light Source and the staff of beamline 19-BM at the Advanced Photon Source for their support. We acknowledge Dr. James Holton, Dr. Mark Robien, Paulene Quigley-Sheldon, Claire O'Neal, Jungwoo Choe, and Daniel Mitchell for assistance with data collection. W.G.J.H. acknowledges the Murdock Charitable Trust for a major equipment grant to the Biomolecular Structure Center at the University of Washington. This work was supported by NIH grants GM49156 to J.J.C. and CA65656 to W.J.G.H.

Received: December 2, 2002
Accepted: January 14, 2003

References

1. Yang, S.W., Burgin, A.B., Jr., Huizenga, B.N., Robertson, C.A., Yao, K.C., and Nash, H.A. (1996). A eukaryotic enzyme that can disjoin dead-end covalent complexes between DNA and type I topoisomerases. Proc. Natl. Acad. Sci. USA *93*, 11534–11539.
2. Strumberg, D., Pilon, A.A., Smith, M., Hickey, R., Malkas, L., and Pommier, Y. (2000). Conversion of topoisomerase I cleavage complexes on the leading strand of ribosomal DNA into 5′-phosphorylated DNA double-strand breaks by replication runoff. Mol. Cell. Biol. *20*, 3977–3987.
3. Pourquier, P., and Pommier, Y. (2001). Topoisomerase I-mediated DNA damage. Adv. Cancer Res. *80*, 189–216.
4. Pommier, Y. (1998). Diversity of DNA topoisomerases I and inhibitors. Biochimie *80*, 255–270.
5. Pouliot, J.J., Yao, K.C., Robertson, C.A., and Nash, H.A. (1999). Yeast gene for a Tyr-DNA phosphodiesterase that repairs topoisomerase I complexes. Science *286*, 552–555.
6. Pouliot, J.J., Robertson, C.A., and Nash, H.A. (2001). Pathways for repair of topoisomerase I covalent complexes in *Saccharomyces cerevisiae*. Genes Cells *6*, 677–687.
7. Vance, J.R., and Wilson, T.E. (2002). Yeast Tdp1 and Rad1-Rad10 function as redundant pathways for repairing Top1 replicative damage. Proc. Natl. Acad. Sci. USA *99*, 13669–13674.
8. Liu, C., Pouliot, J.J., and Nash, H.A. (2002). Repair of topoisomerase I covalent complexes in the absence of the tyrosyl-DNA phosphodiesterase Tdp1. Proc. Natl. Acad. Sci. USA *99*, 14970–14975.
9. Takashima, H., Boerkoel, C.F., John, J., Saifi, G.M., Salih, M.A.M., Armstrong, D., Mao, Y., Quiocho, F.A., Roa, B.B., Nakagawa, M., et al. (2002). Mutation of *TDP1*, encoding a topoisomerase I-dependent DNA damage repair enzyme, in spinocerebellar ataxia with axonal neuropathy. Nat. Genet. *32*, 267–272.
10. Interthal, H., Pouliot, J.J., and Champoux, J.J. (2001). The tyrosyl-DNA phosphodiesterase Tdp1 is a member of the phospholipase D superfamily. Proc. Natl. Acad. Sci. USA *98*, 12009–12014.
11. Davies, D.R., Interthal, H., Champoux, J.J., and Hol, W.G.J. (2002). The crystal structure of human tyrosyl-DNA phosphodiesterase, Tdp1. Structure *10*, 237–248.
12. Koonin, E.V. (1996). A duplicated catalytic motif in a new superfamily of phosphohydrolases and phospholipid synthases that includes poxvirus envelope proteins. Trends Biochem. Sci. *21*, 242–243.
13. Morris, A.J., Engebrecht, J., and Frohman, M.A. (1996). Structure and regulation of phospholipase D. Trends Pharmacol. Sci. *17*, 182–185.
14. Ponting, C.P., and Kerr, I.D. (1996). A novel family of phospholipase D homologues that includes phospholipid synthases and putative endonucleases: identification of duplicated repeats and potential active site residues. Protein Sci. *5*, 914–922.
15. Sapranauskas, R., Sasnauskas, G., Lagunavicius, A., Vikaitis, G., Lubys, A., and Siksnys, V. (2000). Novel subtype of type IIs restriction enzymes. J. Biol. Chem. *275*, 30878–30885.
16. Stuckey, J.A., and Dixon, J.E. (1999). Crystal structure of a phospholipase D family member. Nat. Struct. Biol. *6*, 278–284.
17. Leiros, I., Secundo, F., Zambonelli, C., Servi, S., and Hough, E. (2000). The first crystal structure of a phospholipase D. Struct. Fold. Des. *8*, 655–667.
18. Stanacev, N.Z., and Stuhne-Sekalec, L. (1970). On the mechanism of enzymatic phosphatidylation. Biosynthesis of cardiolipin catalyzed by phospholipase D. Biochim. Biophys. Acta *210*, 350–352.
19. Bruzik, K., and Tsai, M.D. (1984). Phospholipids chiral at phosphorus. Synthesis of chiral phosphatidylcholine and stereochemistry of phospholipase D. Biochemistry *23*, 1656–1661.
20. Raetz, C.R., Carman, G.M., Dowhan, W., Jiang, R.T., Waszkuc, W., Loffredo, W., and Tsai, M.D. (1987). Phospholipids chiral at phosphorus. Steric course of the reactions catalyzed by phosphatidylserine synthase from Escherichia coli and yeast. Biochemistry *26*, 4022–4027.
21. Gottlin, E.B., Rudolph, A.E., Zhao, Y., Matthews, H.R., and Dixon, J.E. (1998). Catalytic mechanism of the phospholipase D superfamily proceeds via a covalent phosphohistidine intermediate. Proc. Natl. Acad. Sci. USA *95*, 9202–9207.
22. Rudolph, A.E., Stuckey, J.A., Zhao, Y., Matthews, H.R., Patton, W.A., Moss, J., and Dixon, J.E. (1999). Expression, characterization, and mutagenesis of the Yersinia pestis murine toxin, a phospholipase D superfamily member. J. Biol. Chem. *274*, 11824–11831.
23. Davies, D.R., Interthal, H., Champoux, J.J., and Hol, W.G.J.

(2002). Insights into substrate binding and catalytic mechanism of human tyrosyl-DNA phosphodiesterase (Tdp1) from vanadate and tungstate-inhibited structures. J. Mol. Biol. *324*, 917–932.
24. Redinbo, M.R., Stewart, L., Kuhn, P., Champoux, J.J., and Hol, W.G.J. (1998). Crystal structures of human topoisomerase I in covalent and noncovalent complexes with DNA. Science *279*, 1504–1513.
25. Inamdar, K.V., Pouliot, J.J., Zhou, T., Lees-Miller, S.P., Rasouli-Nia, A., and Povirk, L.F. (2002). Conversion of phosphoglycolate to phosphate termini on 3′ overhangs of DNA double-strand breaks by the human tyrosyl-DNA phosphodiesterase. J. Biol. Chem. *277*, 27162–27168.
26. Stewart, L., Redinbo, M.R., Qiu, X., Hol, W.G., and Champoux, J.J. (1998). A model for the mechanism of human topoisomerase I. Science *279*, 1534–1541.
27. Been, M.D., Burgess, R.R., and Champoux, J.J. (1984). Nucleotide sequence preference at rat liver and wheat germ type I DNA topoisomerase breakage sites in duplex SV40 DNA. Nucleic Acids Res. *12*, 3097–3114.
28. Parker, L.H., and Champoux, J.J. (1993). Analysis of the biased distribution of topoisomerase I break sites on replicating simian virus 40 DNA. J. Mol. Biol. *23*, 6–18.
29. Smith, C.A., and Rayment, I. (1996). X-ray structure of the magnesium(II)-ADP-vanadate complex of the *Dictyostelium discoideum* myosin motor domain to 1.9 angstrom resolution. Biochemistry *35*, 5404–5417.
30. Rupert, P.B., Massey, A.P., Sigurdsson, S., and Ferre-D'Amare, A.R. (2002). Transition state stabilization by a catalytic RNA. Science *298*, 1421–1424.
31. Otwinowski, Z., and Minor, W. (1997). Processing of X-ray diffraction data collected in oscillation mode. Methods Enzymol. *276*, 307–326.
32. CCP4 (Collaborative Computational Project 4) (1994). The CCP4 suite: programs for protein crystallography. Acta Crystallogr. D *50*, 760–763.
33. McRee, D.E. (1999). XtalView/Xfit–A versatile program for manipulating atomic coordinates and electron density. J. Struct. Biol. *125*, 156–165.
34. Carson, M. (1997). Ribbons. Methods Enzymol. *277*, 493–505.
35. Nicholls, A., Sharp, K.A., and Honig, B. (1991). Protein folding and association: insights from the interfacial and thermodynamic properties of hydrocarbons. Proteins *11*, 281–296.

Accession Numbers

The atomic coordinates and structure factor amplitudes of the Tdp1 quaternary complex with peptide, DNA, and vanadate have been deposited in the Protein Data Bank under ID code 1NOP.